

FEATURE-BASED REAL-TIME AERIAL IMAGE STITCHING AND QUALITY
ASSESSMENT FOR POST-DISASTER APPLICATION

DHANESH A/L KUMARESWARAN

A thesis submitted in fulfilment of the
requirements for the award of the degree of
Master of Philosophy

Faculty of Mechanical Engineering
Universiti Teknologi Malaysia

OCTOBER 2022

ACKNOWLEDGEMENT

In preparing this thesis, I managed to meet many people. Some helped me academically in my research, and some helped keep me sane throughout the pandemic. Firstly, I sincerely appreciate my main thesis supervisor, Ir. Dr.-Ing. Mohd Nazri Bin Mohd Nasir, for encouragement, guidance, criticism, and friendship. I am also very thankful to my co-supervisor, Assoc. Prof. Dr. Muhammad Zulkarnain Bin Abdul Rahman and Dr. Mastura Binti Ab Wahid for their guidance, advice, and motivation. Without my co-supervisor guidance, I would not have completed my algorithm for aerial image stitching.

I am also indebted to Universiti Teknologi Malaysia (UTM) for funding my master's study. Librarians at UTM and lab technicians of the Unmanned Aerial Vehicle lab (UAV LAB) also deserve special thanks for assisting me in conducting the experiments.

I am also indebted to my friends, Haitiswaran Mutharasan, Navinthiran Rajan, Nithyaganeshan Thamocharan, Hanusia Velefly, Tikashini Balasingam, Ranjiitha Singarajan, and Sugeetha Iephran. Unfortunately, it is not possible to list all of them in this limited space. I am grateful to my uncle Lingarajan Anthony for advising me in choosing this research field. I am also indebted to my juniors Arun Rajagopal, Ginesh Raj, and Arvindran Elumalai for helping to be sane throughout the pandemic.

ABSTRACT

In the past, digital maps were created using a photogrammetry framework where the Unmanned Aerial Vehicle (UAV) would collect the aerial images; then, images would be post-processed through commercial software using the Structure From Motion (SFM) method. Creating digital maps has been helpful for remote sensing, especially for studying and observing the terrain. However, one disadvantage of this method of creating digital maps is that it consumes more computational time. Although commercial solutions are widely used, they are not suitable in disaster-affected areas because of the long computational time. Disasters such as earthquakes, floods, and landslides would happen without prior notice, and areas affected by such a disaster would suffer heavy damage. In such a situation, the authorities need an instant digital map to observe the affected areas and decide. Hence, this study focuses on accelerating the creation of a digital map using the real-time image stitching method. Image stitching itself can be divided into feature-based and region-based methods. This study uses a feature-based image stitching method to accelerate the map creation process. This research formulated an image stitching algorithm to stitch aerial images in real-time. A processing speed of 37 frames per second was achieved. The image stitching algorithm was optimized to stitch large areas captured using the multi-grid flight path; a processing speed of 2 frames per second was achieved. Finally, an image selection algorithm was introduced to improve the stitch image quality by 14% and the computational time by 2-fold for a multi-grid flight path. In conclusion, the developed image stitching algorithm can reduce the computational time needed to produce a digital map at the disaster site. Although the developed image stitching algorithm can stitch faster with improved quality, more testing needs to be conducted using aerial images from disaster sites.

ABSTRAK

Pada masa lalu, peta digital dihasilkan menggunakan kerangka fotogrametri dengan menggunakan *Unmanned Aerial Vehicle* (UAV) untuk mengumpul gambar aerial; kemudian, gambar tersebut akan diproses melalui perisian komersial menggunakan kaedah *Structure From Motion* (SFM). Penghasilan peta digital membantu remote sensing terutama untuk kajian dan pemerhatian kawasan. Bagaimanapun salah satu kelemahan dengan kaedah ini dalam menghasilkan peta digital adalah ianya mengambil masa pemrosesan yang lebih. Walaupun penyelesaian komersial digunakan secara meluas, ia tidak sesuai digunakan untuk kawasan yang dilanda bencana kerana masa pemrosesan yang lama. Bencana seperti gempa bumi, banjir, dan tanah runtuh berlaku tanpa amaran awal, dan kawasan yang terkesan dari bencana tersebut akan mengalami kerosakan yang besar. Dalam keadaan seperti itu, pihak berkuasa memerlukan peta digital segera untuk memeliti kawasan terkesan dan membuat keputusan. Oleh itu, kajian ini menumpu kearah penghasilan peta digital pantas menggunakan kaedah berasaskan pencantuman imej masa-nyata. Kaedah pencantuman imej itu sendiri dapat dibahagikan kepada kaedah berasaskan ciri dan berasaskan wilayah. Kajian ini menggunakan kaedah pencantuman imej berasaskan ciri untuk mempercepatkan proses penghasilan peta. Kajian ini merumus algoritma pencantuman imej untuk mencantumkan imej aerial dalam masa-nyata. Masa pemrosesan 37 bingkai sesaat telah dicapai. Algoritma pencantuman imej telah dioptimumkan untuk mencantumkan kawasan luas yang diperolehi menggunakan laluan penerbangan pelbagai grid; kelajuan pemrosesan 2 bingkai sesaat telah dicapai. Akhirnya, algoritma pemilihan imej telah diperkenalkan untuk meningkatkan kualiti imej cantuman sebanyak 14% dan meningkatkan masa pemrosesan sebanyak 2 kali ganda untuk laluan penerbangan pelbagai grid. Kesimpulannya, algoritma pencantuman imej yang dibangunkan dapat mengurangkan masa pemrosesan untuk menghasilkan peta digital di tapak bencana. Walaupun algoritma pencantuman imej yang dibangunkan dapat mencantumkan imej pada kadar yang lebih pantas dengan kualiti yang dipertingkatkan, lebih banyak ujian perlu dijalankan menggunakan imej aerial dari tapak bencana.

TABLE OF CONTENTS

	TITLE	PAGE
	DECLARATION	iii
	DEDICATION	iv
	ACKNOWLEDGEMENT	v
	ABSTRACT	vi
	ABSTRAK	vii
	TABLE OF CONTENTS	viii
	LIST OF TABLES	xi
	LIST OF FIGURES	xiii
	LIST OF ABBREVIATIONS	xvii
CHAPTER 1	INTRODUCTION	1
	1.1 Problem Background	1
	1.2 Problem Statement	6
	1.3 Purpose Statement	7
	1.4 Objectives	7
	1.5 Scope and Limitation	8
	1.6 Research Contribution	9
	1.7 Significance of Research	9
	1.8 Research Flowchart	10
	1.9 Organization of Thesis	10
CHAPTER 2	LITERATURE REVIEW	13
	2.1 Introduction	13
	2.2 Materials for Image Stitching	13
	2.2.1 Roles of UAV in Image Stitching	13
	2.2.2 Roles of Camera in Image Stitching	16
	2.2.3 Role of Communicational Link in Image Stitching	21

2.2.4	Role of Computer Specification in Image Stitching	22
2.3	Image Stitching Algorithm	25
2.3.1	General Pipeline for Image Stitching	25
2.3.2	Image Preprocessing	33
2.3.1	Real-time Aerial Image Stitching Approaches	36
2.4	Image Quality Assessment	39
2.4.1	Reduced-Reference Evaluation	39
2.4.2	No-Reference Evaluation	42
2.5	UAVs in Disaster	43
2.6	Summary	47
CHAPTER 3	RESEARCH METHODOLOGY	49
3.1	Introduction	49
3.2	Path Planning	50
3.3	Materials	53
3.3.1	UAV Specification	53
3.3.2	Computer Specification	54
3.3.3	Study Location	54
3.3.4	Dataset	55
3.4	Research Procedure Flowchart	57
3.4.1	Method for Experiment I	58
3.4.2	Method for Experiment II	61
3.4.3	Method for Experiment III	63
3.5	Research Timeline	66
CHAPTER 4	RESULTS AND DISCUSSION	67
4.1	Introduction	67
4.2	Computational Time for Stitching Aerial Images in a Straight Line Trajectory	67
4.3	Assessment of Stitched Image Quality for Straight-Line Trajectory	69
4.4	Computational Time of Stitching Aerial Images in a Multigrid Flight Trajectory	71

LIST OF TABLES

TABLE NO.	TITLE	PAGE
Table 1.1	Comparison between commercial software and image stitching proposed by (Bu et al., 2016) .Note: The computational time is in minutes.	5
Table 1.2	Comparison between trial duration between commercial software (Alidoost and Arefi, 2017)	5
Table 2.1	Compares UAV type, flight speed, payload, and distance traveled for real-time image stitching.	16
Table 2.2	A comparison of camera parameters specification chosen by authors. For example, A clear pattern of using a CMOS camera is established among the authors.	20
Table 2.3	Compares computational specifications (RAM, GPU, and CPU) with the computational time, respective image resolution, and total images. For example, parallel processing has increased the image processing speed drastically.	24
Table 2.4	A comparison of Image Stitching Algorithm. Each author's proposed algorithm and recommendation have been compared in this table to obtain a clear overview.	28
Table 2.5	Pre-processing approaches with and without GPS data to reduce misalignment of aerial images	34
Table 2.6	Comparison between real-time image stitching approaches.	37
Table 3.1	Details each dataset's sequences on maximum altitude, trajectory length, and the number of images. (/) indicates the information was not available.	56
Table 3.2	Gantt chart of Work Progress	66
Table 4.1	Comparison between the proposed method and other findings. The red highlight represents the fastest stitching achieved in the particular dataset.	72
Table 4.2	Comparison of the area (km ²) covered in a second. The red highlight represents the fastest stitching achieved in the particular dataset.	73
Table 4.3	Comparison between the proposed method and proposed method combined with image selection algorithm. The	

Figure 2.6	Image (a) captured when the Siemens star is static using a global shutter camera. Image (b) is captured when the Siemens star rotates clockwise using a rolling shutter resulting in a distorted image (Zhou et al., 2020).	20
Figure 2.7	There are several types of drone communication (cellular communication, drone communication, satellite communication, and ground communication) (Yaacoub et al., 2020)	22
Figure 2.8	The comparison between GPU and CPU processing time with different image resolutions (Nan et al., 2010)	23
Figure 2.9	Type of 2D image transformation	31
Figure 2.10	General framework of reduced-reference evaluation (Zhai and Min, 2020)	42
Figure 2.11	General framework of no-reference evaluation (Xu et al., 2017)	43
Figure 2.12	The risk calculation includes hazard, exposure, and vulnerability. (Tostevin, 2014).	44
Figure 2.13	Weather condition (icing, crosswinds, high winds, heavy rain, and fog) that affects the UAV flight condition (Zieliński, 2017)	45
Figure 3.1	General workflow of experiment	49
Figure 3.2	The path planning for image stitching calculation. (Reworked from Scholarin and co-workers) (Sholarin and Awange, 2015).	52
Figure 3.3	An overview of research, where the captured aerial data (image/video format) are sent to the ground station to be processed in real-time. The image is stitched in real-time at the ground station.	53
Figure 3.4	DJI Mavic Mini 2 was deployed in this study to collect the aerial images. The DJI Mavic Mini 2 is a quadcopter with 249g weight with a camera of 12 MP resolution. Source: https://www.dji.com/mini-2?site=brandsite&from=eol_mavic-mini	54
Figure 3.5	Selected study location with an area of 0.07 km ² . The study location is longitude (103.6414187-103.6418915) and latitude (1.5537941-1.5540763). The red box indicated the location with building only, the blue box represented the locations with nature only, and the green box represented the location with buildings and nature	55
Figure 3.6	Flightpath for NPU and Pix4D dataset. () refers to forward motion and () backward motion.	56

Figure 3.7	The flowchart used to conduct the research	57
Figure 3.8	Real-time image stitching algorithm flowchart where IK represent the first frame and $IK + 1$ represent the second frame. Both the frames undergo feature detection, and the homography matrix is estimated using the RANSAC algorithm by removing outliers. Then the perspective transform occurs where the second frame is used as a reference to transform the first frame according to the second frame. Then the first frame is wrapped according to the second frame and stitched together as stitched image, IS . Finally, the second frame is set as the first frame to continue the iterative image stitching process. Once a stitched image is present in the first frame is substituted with the stitched image.	58
Figure 3.9	Aerial image stitching using the algorithm in Figure 3.8. The aerial image suffered from distortion, making it not appealing for observation of decision-making.	60
Figure 3.10	The revised algorithm from Figure 3.8. In this algorithm, instead of using the second frame as a reference frame, the first frame is used as a reference frame to estimate the homography. Furthermore, the addition of a homography matrix is performed to ease the process of image wrapping	60
Figure 3.11	The change in homography between the first algorithm (algorithm in Figure 3.8) and the homography improved algorithm (algorithm in Figure 3.10). Homography improved algorithm exhibited a minor change in homography than the first algorithm along the image stitching process. Besides, there is a high error accumulation using the first algorithm, making complex computation (between frames 301 to 351)	61
Figure 3.12	Stitched image using the algorithm in Figure 3.10. See (https://www.youtube.com/watch?v=hnNbLXlp6eg) for the output of the improvised algorithm. The aerial footage was taken at 50 meters altitude and a UAV speed of 5 m/s using a DJI mini drone. A total distance of 400m was covered in this footage.	61
Figure 3.13	The stitched image using local homography. The red circle indicated the misalignment when stitching a multi-grid flight path. The section in the circle was supposed to be stitched near the green circle, as in Figure 3.14.	63
Figure 3.14	The stitched image using global homography. See the image stitching of the multi-grid flight path (https://youtu.be/bMsjp2ga0no).	63

Figure 3.15	Overview of proposed image selection algorithm framework to reduce the redundancy of aerial images. Images with the highest matched features are only deployed to the next stage (image stitching). The red line represents the matched features between image three and image one, and the green line represents the matched line between image two and image one. The dotted box indicates a window size of three deployed in the study.	65
Figure 4.1	Compares computational time between ORB, AKAZE, SIFT, and BRISK. The number of skipped frames (NSF) was calculated by dividing the total frames of drone video by the frames used. For example, the NSF value is 1, which means all frames were used accordingly.	68
Figure 4.2	The number of skip frames versus RMSE, PSNR, SSIM, and BRISQUE SCORE. A higher value of PSNR values explains less noise in the image than in the reference image. The SSIM value ranges from 0 to 1 to describe the structural similarity between both images, where 1 denotes a similar image is detected. Besides, higher values of the BRISQUE score denote more distortion in the stitched image. A higher PSNR value reveals less noise than in the reference image.	70
Figure 4.3	Graphical illustration of data in Table 4.1. A comparison between the proposed method and other authors' findings.	73
Figure 4.4	Comparison plot of features obtained in 5 different datasets. The upper line represents the maximum value, the middle line represents the mean value, and the lower line indicates the lower limit. The red plot shows the feature obtained using the proposed algorithm with the image selection algorithm	81
Figure 4.5	Aerial images from Rock S.O.D.A. RGB camera dataset. (a) The flight path for capturing aerial images. (b) Mosaic image using Pix4D. (c) Mosaic image using the proposed algorithm	82
Figure 4.6	Aerial images from Rock S.O.D.A. RGB camera dataset. (a) The flight path for capturing aerial images. (b) Mosaic image using Pix4d. (c) Mosaic image using the proposed algorithm	82

LIST OF ABBREVIATIONS

BF Matcher	-	Brute Force Matcher
BLINDS	-	Blind Image Notator Using DCT Statistics
BOW	-	Bag Of Words
BRIEF	-	Binary Robust Independent Elementary Features
BRISK	-	Binary Robust Invariant Scalable Keypoints
BRISQUE	-	Blind/Referenceless Image Quality Assessment
CAAM	-	Civil Aviation Authority of Malaysia
CCD	-	Charge-Coupled Device
CMOS	-	Complementary Metal Oxide Semiconductor
CPU	-	Computational Processing Unit
FAST	-	Features from Accelerated Segment Test
GCP	-	Ground Control Point
GNSS	-	Global Navigation Satellite System
GPS	-	Global Position System
GPU	-	Graphics Processing Unit
GSD	-	Ground Sample Distance
INS	-	Inertial Navigation Sensors
ISO	-	International Organisation for Standardization
KD TREE	-	K-Decision Tree
KNN	-	K- Nearest Neighbour
LIDAR	-	Light Detection and Ranging
MSE	-	Mean Square Error
MCMC	-	Malaysian Communication and Multimedia Commission
ORB	-	Oriented fast and Rotated Brief
PPK	-	Post-Processing Kinematics
PSNR	-	Peak Signal to Noise Ratio
RAM	-	Random Access Memory
RANSAC	-	RANdom SAmples Consensus
RC	-	Remote Controlled
RMSE	-	Root Mean Square Error

- ROA - Remotely Operated Aircraft
- RPV - Remotely Piloted Vehicle
- RTK - Real-time Kinematics
- UAV - Unmanned Aerial Vehicle
- UVS - Unmanned Vehicle System

CHAPTER 1

INTRODUCTION

1.1 Problem Background

A disaster is an unpredicted event that causes significant damage in terms of loss of life, destruction, and drastic environmental changes; this event can be divided into natural or man-made (Restas, 2015; Sathish Kumar et al., 2020). Natural disasters include earthquakes, floods, hurricanes, and landslides; man-made disasters are construction accidents, nuclear leaks, and explosions (Sathish Kumar et al., 2020). A disaster can be scaled into different scales depending on the affected area, affected population, and spreading time (see Figure 1.1 and Figure 1.2) (Restas, 2015). Between 2002 to 2011, about 107,000 people were killed, and 268 million people were victims of natural disasters worldwide annually (Tanzi et al., 2014). Hence, when a natural disaster occurs, it is necessary to quickly and effectively organize a disaster management operation to reduce life and economic losses; without such management, the disaster victims will undergo drastic losses (Sathish Kumar et al., 2020; Tanzi et al., 2014).

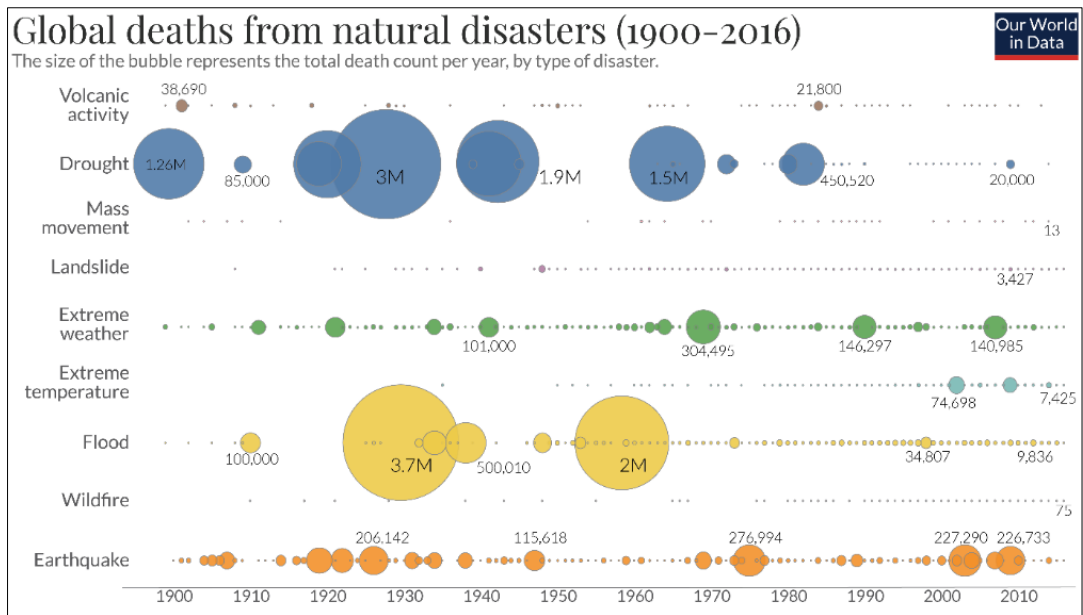


Figure 1.1 From the year 1900 to the year 2010, people died due to natural disasters. Source: Our World in Data <https://ourworldindata.org/natural-disaster>.

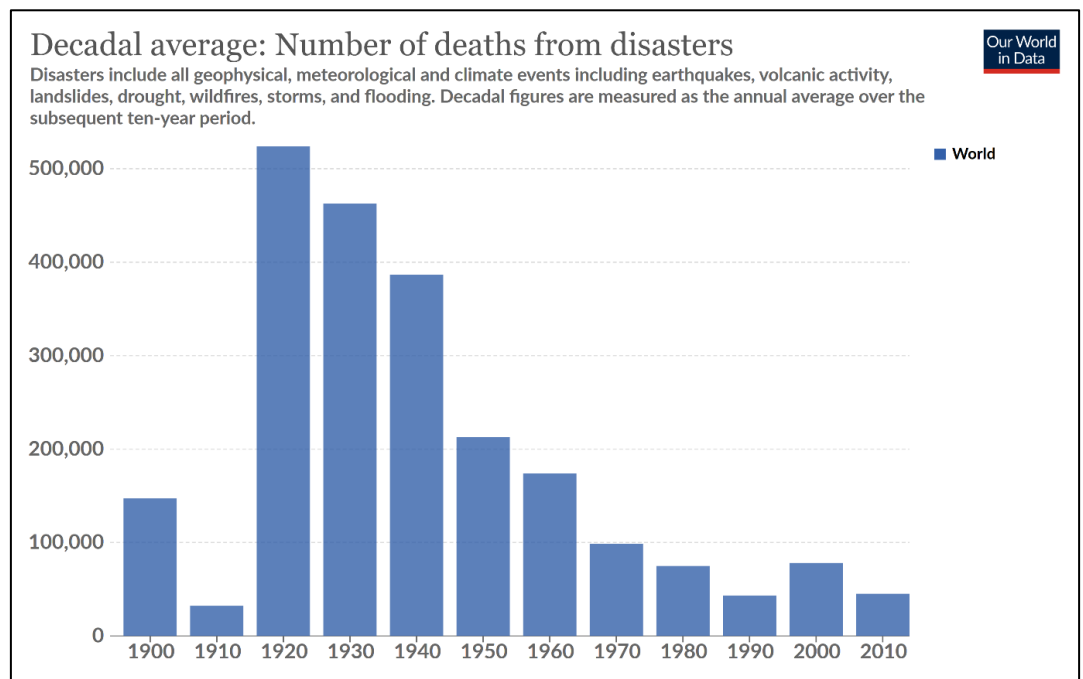


Figure 1.2 Death people annually due to natural disasters. Source: Our World in Data <https://ourworldindata.org/natural-disasters>.

In the past, digital maps for remote sensing and surveillance are created using photogrammetric workflow (a process of developing a three-dimensional (3D) model using two-dimensional (2D) images), which uses the structure from motion (SFM) method (a technique of estimating the camera poses based on the 2D image) (Fanta-Jende et al., 2020; Hein et al., 2019). The aerial images are acquired using an Unmanned Aerial Vehicle (UAV) in the photogrammetry workflow. Then the aerial images undergo post-processing using the commercial software after the UAV lands (Hein et al., 2019). Much commercial software (Pix4d, Agisoft Metashape, and 3D Survey) was developed using the SFM method for creating a digital map (Fanta-Jende et al., 2020); the disadvantage of the SFM method is that it has a prolonged computational time (see Table 1.1) (Bu et al., 2016; Hein et al., 2019). Besides, the commercial software is imposed with charges once the free trial period has ended (see Table 1.2) (Alidoost and Arefi, 2017).

Since the authorities require an instant digital map to decide, the traditional method is unsuitable for the response stage. As a solution, image stitching has been used to provide a faster digital map (see Figure 1.4) (Fanta-Jende et al., 2020; Hein et al., 2019). Image stitching combines overlapping images with similar features into one large image (see Figure 1.4) (Abdelkrim et al., 2018; Nocerino et al., 2020; Vaidya and Gandhe, 2018; Wang and Yang, 2020). An instant observation image is needed for the authorities to decide and calculate the risk in the response stage. However, the commercial software cannot meet the computational requirement. Hence, in this research, the image stitching method will be deployed to produce a fast observation image for disaster management authorities.

Table 1.1 Comparison between commercial software and image stitching proposed by (Bu et al., 2016) .Note: The computational time is in minutes.

Sequence Id	Frames	Keyframes	Bu & Co-workers	Pix4D	Photoscan
1	28493	337	15.84	107.05	153.62
2	18869	395	10.49	52.62	334.73
3	19371	482	16.44	83.75	683.98
4	13983	457	9.32	140.08	532.38
5	12744	471	8.49	127.73	563.57
6	4585	648	2.39	154.77	999.67
7	16969	406	11.31	132.07	360.70
8	16292	221	10.86	72.13	145.52
9	14776	393	10.36	102.83	462.32

Table 1.2 Comparison between trial duration between commercial software (Alidoost and Arefi, 2017)

Software	Trial License Validation (day)
3D Survey	15
Agisoft	30
Pix4Dmapper	7
SURE	4

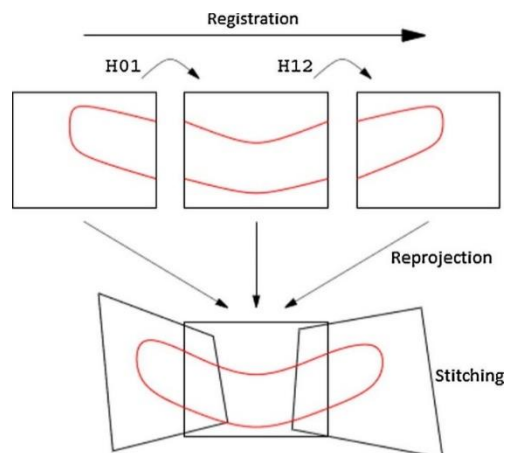


Figure 1.4 Process of Image stitching (registration, reprojection, and stitching). ‘H01’ and ‘H12’ refer to homography estimation (Ghosh and Kaabouch, 2016).

1.2 Problem Statement

Currently, digital maps are generated using commercial software such as Pix4D and Agisoft (Fanta-Jende et al., 2020). This commercial software generates a digital map using the photogrammetry framework; one drawback of using the commercial software is that it consumes prolonged computational time depending on the area size and resolution of aerial images (Bu et al., 2016; Hein et al., 2019). Since the commercial software needs a prolonged time to generate a digital map, it is not suitable to be deployed in disaster areas because at the disaster site; the disaster management authorities require a real-time digital map or observatory image to plan the intervention during the response stage (Bu et al., 2016; de Lima et al., 2020; Fanta-Jende et al., 2020). Hence, to solve this problem, Bu and co-workers suggested deploying the image stitching algorithm to generate the digital map faster (see Table 1.1) (Bu et al., 2016).

Although many studies have been conducted on the photogrammetry workflow, scant attention has been given to producing a faster digital map using the image stitching method. A few works have been conducted to create digital maps using the image stitching method.

Since aerial image stitching is still an emerging research niche, previous work has identified a few gaps. Fanta and co-workers established a near real-time image stitching algorithm, but the authors found that stitch quality and processing time need improvement (Fanta-Jende et al., 2020). A similar problem was faced by Hein and co-workers, where the quality of the stitch map needs to be improved by improving the stitch quality and positional accuracy by geo-referencing (Hein et al., 2019). De Lima and co-workers created a real-time image stitching algorithm; however, the algorithm consumes more time with the high-resolution image (4MP) in real-time (De Lima and Martinez-Carranza, 2017). Besides, the authors also suggested that real-time image stitching can be improved by incorporating GPS coordinates in image registration to avoid drift error (change of flight trajectory due to crosswind) (de Lima et al., 2020).

By reviewing the gaps in the literature, this research will focus on developing an algorithm to stitch aerial images in real-time and improve the visual quality of stitched images to aid the disaster management authorities. Real-time image processing is the image processing speed equivalent to the source (video) speed. For example, if the video has 25 fps, each frame must be processed within 0.04s to achieve real-time speed (Burgos-Artizzu et al., 2011). Disaster management authorities can plan the intervention route faster by deploying a real-time image stitching algorithm.

1.3 Purpose Statement

This research aims to formulate an algorithm to stitch aerial images faster and improve the stitch quality. A faster image stitching algorithm will be developed to reduce computational time. The quality of the stitched image will be assessed and improved to optimize the quality.

1.4 Objectives

This research aims to reduce the computational time of creating an observatory image for disaster-affected areas.

1. To formulate an algorithm for real-time aerial image stitching.
2. To optimize the algorithm to stitch aerial images in a multi-grid flight path.
3. To quantify the visual quality of the stitched image and optimize the quality of the stitched image.

1.5 Scope and Limitation

The research focuses on feature-based image stitching. Hence image stitching requires areas rich with features (a feature is a distinct pattern in an image, such as corners, blobs, and edges)(Szeliski, 2007; Wang and Yang, 2020). The maximum distance covered in this research is 150m only from the UAV lab at UTM due to the limitation of the communicational link between the UAV and the ground station. In addition, the mobility of the ground station is limited; hence the research is conducted at a 150m distance radius from the UAV lab. Besides rules from the Civil Aviation Authorities of Malaysia (CAAM), rules limit that UAVs should not fly beyond the visual line of sight (CAAM: UAS 02/2019 (https://www.caam.gov.my/wp-content/uploads/2021/03/CAAM-Drone_Requirement_2020.pdf)).

On the other hand, a maximum altitude of 120m will only be tested in this research because CAAM does not allow the flight of UAVs more than 400 feet (121.92m) from the earth's surface. A commercial UAV (DJI mini 2) was utilized in this research because the custom-made drone requires a special permit to fly. In addition, UTM is located in a no-fly zone due to the presence of Senai International Airport.

Besides, this research focuses on capturing aerial images by facing the camera at the nadir line to maintain a constant Ground Sample Distance (GSD) (not including terrain relief). In the research, only one camera is used for real-time image stitching. This research does not include multi-camera image stitching because of increased payload and cost. Latency by communicational link is not covered in this research because the speed and strength of the communicational link depend on the distance from the cellular tower. Besides, this research intends to speed up the image processing time. Since this research intends to create an observation image for the authorities, geo-referencing and geo-rectification are omitted.

In addition, the OpenCV library in a python environment was deployed to formulate the algorithm in this research. The OpenCV library was deployed because it was equipped with tools for image processing. Besides, the python environment was able to import the OpenCV library.

1.6 Research Contribution

A real-time image stitching algorithm for observing the disaster-affected areas was developed to solve the computational complexity in commercial software. The significance and contribution of this research are listed :

1. Developed an image stitching algorithm for disaster-affected areas.
2. Proposed an image selection algorithm to optimize the visual quality of stitch images.
3. Stitched aerial images with a multi-grid flight path at a processing speed.

1.7 Significance of Research

This research developed a faster observation image through the image stitching method; this would help the authorities, such as NADMA, to make the decision easier and faster. Since the visual quality of the observatory image was improved, it helped the authority's decision-making process more manageable. The outcome of this research can also be applied in other fields, such as forest monitoring and surveillance, by easing the forest inventory update process. In addition, the proposed method will be helpful for a country like Malaysia (especially the Kelantan river basin) since frequent flooding occurs due to monsoon winds and heavy rains (Chan et al., 2016). In addition, this research is multidisciplinary by consisting of many fields together (computer vision, drone technology, and remote sensing)

1.8 Research Flowchart

The following is the workflow of the research to achieve the respective objective.

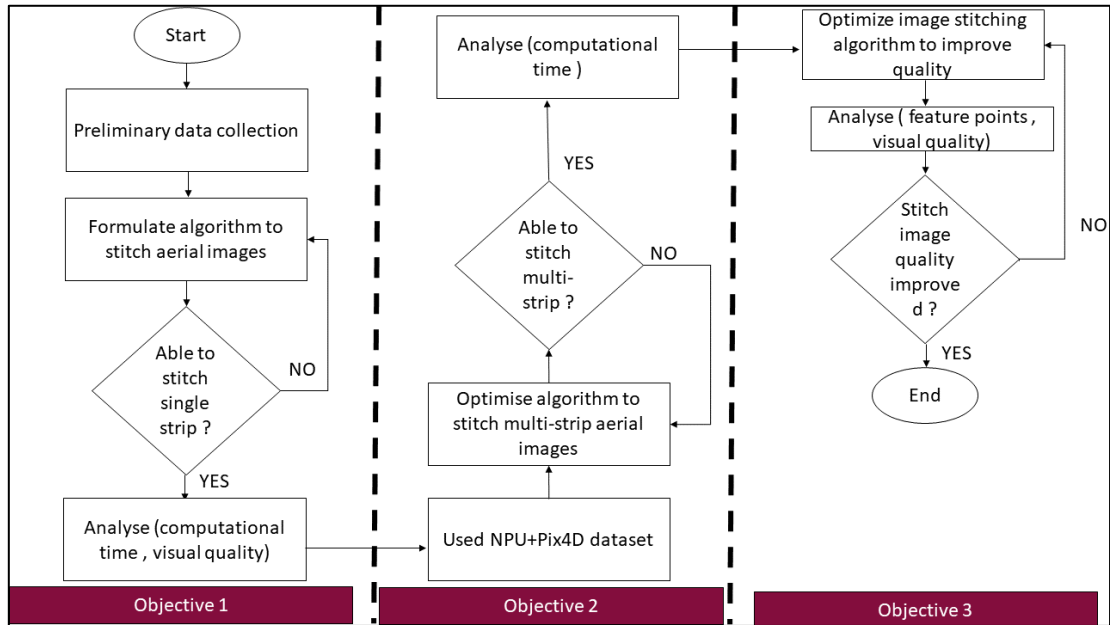


Figure 1.5 Flowchart representing the workflow to achieve the respective objective.

1.9 Organization of Thesis

The organization of the thesis are as follows:

- (a) Chapter 2: The material for image stitching, algorithm, and quality assessment of stitched images will be discussed in detail using prior work from other authors as a reference in this chapter.
- (b) Chapter 3: A detailed discussion of the image stitching methodology will be discussed in this chapter. This section will be subdivided into a research procedure flowchart, experimental setup, and research timeline.

- (c) Chapter 4: In this chapter, a discussion on the results from the image stitching algorithm for a straight-line trajectory are discussed in depth. Then, the results from the image stitching algorithm for the multi-grid flight path are discussed in this chapter.
- (d) Chapter 5: The conclusion and future works for the research are discussed in this chapter.

REFERENCES

1. Abdelhafiz, A. (2009). 'Integrating Digital Photogrammetry and Terrestrial Laser Scanning'. (PHD). Assiut University
2. Abdelkrim, N., Atmane, K., & Houari, S. (2018). 'Quantitative Analysis of Real-Time Image Mosaicing Algorithms'. Paper presented at the *International Conference on Systems, Signals, and Image Processing*.
3. Aber, J. S., Marzloff, I., Ries, J. B., & Aber, S. E. W. (2019). 'Chapter 6 - Cameras for SFAP'. In J. S. Aber, I. Marzloff, J. B. Ries, & S. E. W. Aber (Eds.), *Small-Format Aerial Photography and UAS Imagery (Second Edition)* (pp. 77-92): *Academic Press*.
4. Adel, E., Elmogy, M., & El-Bakry, H. (2014). 'Real Time Image Mosaicing System Based on Feature Extraction Techniques'. Paper presented at the *9th IEEE International Conference on Computer Engineering and Systems, ICCES 2014*.
5. Ahmad, M. I., Ab. Rahim, M. H., Nordin, R., Mohamed, F., Abu-Samah, A., & Abdullah, N. F. (2021). 'Ionizing radiation monitoring technology at the verge of internet of things'. *Sensors*, 21(22).
6. Alidoost, F., & Arefi, H. (2017). 'Comparison of UAS-Based Photogrammetry Software for 3d Point Cloud Generation: A Survey Over A Historical Site'. *ISPRS Ann. Photogramm. Remote Sens. Spatial Inf. Sci.*, IV-4/W4, 55-61.
7. Avola, D., Cinque, L., Foresti, G. L., & Pannone, D. (2020). 'Homography VS Similarity Transformation In Aerial Mosaicking: Which Is The Best At Different Altitudes?'. *Multimedia Tools and Applications*, 79(25-26), 18387-18404.
8. Avola, D., Foresti, G. L., Martinel, N., Micheloni, C., Pannone, D., & Piciarelli, C. (2017) Real-time incremental and geo-referenced mosaicking by small-scale uavs. In: *Vol. 10484 LNCS. Lecture Notes in Computer Science (including subseries Lecture Notes in Artificial Intelligence and Lecture Notes in Bioinformatics)* (pp. 694-705).

9. Battulwar, R., Winkelmaier, G., Valencia, J., Naghadehi, M. Z., Peik, B., Abbasi, B., Parvin, B., & Sattarvand, J. (2020). 'A Practical Methodology for Generating High-Resolution 3D Models of Open-Pit Slopes Using UAVs: Flight Path Planning and Optimization'. *Remote Sensing*, 12(14).
10. Berie, H. T., & Burud, I. (2018). 'Application of unmanned aerial vehicles in earth resources monitoring: focus on evaluating potentials for forest monitoring in Ethiopia'. *European Journal of Remote Sensing*, 51(1), 326-335.
11. Birk, A., Wiggerich, B., Bülow, H., Pflingsthor, M., & Schwertfeger, S. (2011). 'Safety, Security, and Rescue Missions with an Unmanned Aerial Vehicle (UAV)'. *Journal of Intelligent & Robotic Systems*, 64(1), 57-76.
12. Botterill, T., Mills, S., & Green, R. (2010, 8-9 Nov. 2010). 'Real-Time Aerial Image Mosaicing'. Paper presented at the *2010 25th International Conference of Image and Vision Computing New Zealand*.
13. Bu, S., Zhao, Y., Wan, G., & Liu, Z. (2016). 'Map2dfusion: Real-Time Incremental UAV Image Mosaicing Based On Monocular Slam'. Paper presented at the *IEEE International Conference on Intelligent Robots and Systems*.
14. Burgos-Artizzu, X. P., Ribeiro, A., Guijarro, M., & Pajares, G. (2011). 'Real-Time Image Processing For Crop/Weed Discrimination In Maize Fields'. *Computers and Electronics in Agriculture*, 75(2), 337-346.
15. Carvalho, P., Santos, A., Dourado, A., & Ribeiro, B. (2002). 'Radiometric Image Correction With Automatic Model Selection'. Paper presented at the *IFAC Proceedings Volumes (IFAC-PapersOnline)*.
16. Chan, N. W., Ku-Mahamud, K. R., & Abd Karim, M. Z. (2016). 'Assessing different types of flood losses in Kelantan state in Malaysia during the December 2014 flood'.
17. Colomina, I., & Molina, P. (2014). 'Unmanned Aerial Systems for Photogrammetry and Remote Sensing: A Review'. *ISPRS Journal of Photogrammetry and Remote Sensing*, 92, 79-97.
18. De Lima, R., & Martinez-Carranza, J. (2017). 'Real-Time Aerial Image Mosaicing Using Hashing-Based Matching'. Paper presented at the *2017 Workshop on Research, Education and Development of Unmanned Aerial Systems, RED-UAS 2017*.

19. de Lima, R., Cabrera-Ponce, A. A., & Martinez-Carranza, J. (2020). 'Parallel Hashing-Based Matching for Real-Time Aerial Image Mosaicing'. *Journal of Real-Time Image Processing*.
20. Dehbi, Y., Klingbeil, L., & Plümer, L. (2020). 'UAV Mission Planning for Automatic Exploration and Semantic Mapping'. *ISPRS - International Archives of the Photogrammetry, Remote Sensing and Spatial Information Sciences, XLIII-B1-2020*, 521-526.
21. Dissanayake, V., Herath, S., Rasnayaka, S., Seneviratne, S., Vidanaarachchi, R., & Gamage, C. (2015). 'Quantitative and Qualitative Evaluation of Performance and Robustness of Image Stitching Algorithms'.
22. Eisenbeiss, H. (2008). 'The Autonomous Mini Helicopter: A Powerful Platform for Mobile Mapping'. *Int. Arch. Photogramm. Remote Sens. Spatial Inf. Sci.*, XXXVII.
23. Fanta-Jende, P., Steininger, D., Bruckmüller, F., & Sulzbachner, C. (2020). 'A Versatile UAV Near Real-Time Mapping Solution for Disaster Response - Concept, Ideas and Implementation'. Paper presented at the *International Archives of the Photogrammetry, Remote Sensing and Spatial Information Sciences - ISPRS Archives*.
24. Ghosh, D., & Kaabouch, N. (2016). 'A Survey on Image Mosaicing Techniques'. *Journal of Visual Communication and Image Representation*, 34, 1-11.
25. Ghosh, D., Park, S., Kaabouch, N., & Semke, W. (2012, 6-8 May 2012). 'Quantitative Evaluation of Image Mosaicing in Multiple Scene Categories'. Paper presented at the *2012 IEEE International Conference on Electro/Information Technology*.
26. Hashim, K. A., Ahmad, A., Samad, A. M., NizamTahar, K., & Udin, W. S. (2012). 'Integration of Low Altitude Aerial & Terrestrial Photogrammetry Data in 3D Heritage Building Modeling'. Paper presented at the *Proceedings - 2012 IEEE Control and System Graduate Research Colloquium, ICSGRC 2012*.
27. Hein, D., Kraft, T., Brauchle, J., & Berger, R. (2019). 'Integrated UAV-based real-time mapping for security applications'. *ISPRS International Journal of Geo-Information*, 8(5).

28. Herwitz, S. R., Johnson, L. F., Dunagan, S. E., Higgins, R. G., Sullivan, D. V., Zheng, J., Lobitz, B. M., Leung, J. G., Gallmeyer, B. A., Aoyagi, M., Slye, R. E., & Brass, J. A. (2004). 'Imaging from an Unmanned Aerial Vehicle: Agricultural Surveillance and Decision Support'. *Computers and Electronics in Agriculture*, 44(1), 49-61.
29. Jiang, H., Jiang, G., Yu, M., Zhang, Y., Yang, Y., Peng, Z., Chen, F., & Zhang, Q. (2021). 'Cubemap-Based Perception-Driven Blind Quality Assessment for 360-degree Images'. *IEEE Transactions on Image Processing*, 30, 2364-2377.
30. Kainth, K., & Singh, B. (2020). 'Analysis of CCD and CMOS Sensor Based Images from Technical and Photographic Aspects'. Available at SSRN 3559236.
31. Kedzierski, M., Wierzbicki, D., Sekrecka, A., Fryskowska, A., Walczykowski, P., & Siewert, J. (2019). 'Influence of Lower Atmosphere on the Radiometric Quality of Unmanned Aerial Vehicle Imagery'. *Remote Sensing*, 11(10).
32. Kern, A., & Bobbe, M. (2016). 'Towards a Real-Time Image Mosaicing Solution'. Paper presented at the *IMAV 2016*, Beijing.
33. Khan, A., Gupta, S., & Gupta, S. K. (2020). 'Multi-hazard disaster studies: Monitoring, detection, recovery, and management, based on emerging technologies and optimal techniques'. *International Journal of Disaster Risk Reduction*, 47.
34. Kim, J., Kim, T., Shin, D., & Kimb, S. H. (2016). 'Robust Mosaicking of UAV Images with Narrow Overlaps'. Paper presented at the *International Archives of the Photogrammetry, Remote Sensing and Spatial Information Sciences - ISPRS Archives*.
35. Lebourgeois, V., Bégué, A., Labbé, S., Mallavan, B., Prévot, L., & Roux, B. (2008). 'Can Commercial Digital Cameras be Used as Multispectral Sensors? A Crop Monitoring Test'. *Sensors*, 8(11), 7300-7322.
36. Lee, V., Kim, C., Chhugani, J., Deisher, M., Kim, D., Nguyen, A., Satish, N., Smelyanskiy, M., Chennupaty, S., Hammarlund, P., Singhal, R., & Dubey, P. (2010). 'Debunking the 100x GPU Vs. CPU Myth: An Evaluation Of Throughput Computing on CPU and GPU'. *ACM SIGARCH Computer Architecture News*, 38, 451-460.

37. Liu, X., Tan, Y. H., & Chen, B. M. (2018, 18-21 Nov. 2018). 'Adaptive Weight Multi-Band Blending Based Fast Aerial Image Stitching and Mapping'. Paper presented at the *2018 15th International Conference on Control, Automation, Robotics and Vision (ICARCV)*.
38. Lowe, D. G. (2004). 'Distinctive Image Features from Scale-Invariant Keypoints'. *International Journal of Computer Vision*, *60*(2), 91-110.
39. Mittal, A., Moorthy, A. K., & Bovik, A. C. (2012). 'No-Reference Image Quality Assessment in the Spatial Domain'. *IEEE Transactions on Image Processing*, *21*(12), 4695-4708.
40. Mukherjee, D., Jonathan Wu, Q. M., & Wang, G. (2015). 'A Comparative Experimental Study of Image Feature Detectors and Descriptors'. *Machine Vision and Applications*, *26*(4), 443-466.
41. Nan, Z., Yun-shan, C., & Jian-li, W. (2010, 27-29 March 2010). 'Image Parallel Processing Based on GPU'. Paper presented at the *2010 2nd International Conference on Advanced Computer Control*.
42. Nocerino, E., Menna, F., Chemisky, B., & Drap, P. (2020). '3D Sequential Image Mosaicing for Underwater Navigation and Mapping'. *ISPRS - International Archives of the Photogrammetry, Remote Sensing and Spatial Information Sciences*, *XLIII-B2-2020*, 991-998.
43. O'Connor, J., Smith, M. J., & James, M. R. (2017). 'Cameras and Settings for Aerial Surveys in the Geosciences: Optimising Image Data'. *Progress in Physical Geography*, *41*(3), 325-344.
44. Papić, V., Šolić, P., Milan, A., Gotovac, S., & Polić, M. (2021). 'High-Resolution Image Transmission from UAV to Ground Station for Search and Rescue Missions Planning'. *Applied Sciences (Switzerland)*, *11*(5), 1-19.
45. Peng, X., Xianpeng, L., Chao, G., Zan, Z., Chunxiao, G., & Qiongxin, L. (2013, 2013/03). 'A Real-time Stitching Algorithm for UAV Aerial Images'. Paper presented at the *Conference of the 2nd International Conference on Computer Science and Electronics Engineering (ICCSEE 2013)*.
46. Pham, N. T., Park, S., & Park, C. S. (2021). 'Fast and Efficient Method for Large-Scale Aerial Image Stitching'. *IEEE Access*, *9*, 127852-127865.
47. Remondino, F., Barazzetti, L., Nex, F., Scaioni, M., & Sarazzi, D. (2011). 'UAV Photogrammetry for Mapping and 3d Modeling - Current Status and

- Future Perspectives'. *International Conference on Unmanned Aerial Vehicle in Geomatics (Uav-G)*, 38-1(C22), 25-31.
48. Restas, A. (2015). 'Drone Applications for Supporting Disaster Management'. *World Journal of Engineering and Technology*, 03, 316-321.
 49. Restas, A. (2018). 'Water Related Disaster Management Supported by Drone Applications'. *World Journal of Engineering and Technology*, 06, 116-126.
 50. Réstas, A. (2006). 'The Regulation Unmanned Aerial Vehicle of the Szendro Fire Department Supporting Fighting Against Forest Fires 1st in the World'. *Forest Ecology and Management S*, 234, S233.
 51. Rizk, M., Mroue, A., Farran, M., & Charara, J. (2020). 'Real-Time SLAM Based on Image Stitching for Autonomous Navigation of UAVs in GNSS-Denied Regions'. Paper presented at the *Proceedings - 2020 IEEE International Conference on Artificial Intelligence Circuits and Systems, AICAS 2020*.
 52. Sathish Kumar, J., Kumar, S., Choksi, M., & Zaveri, M. A. (2020). 'Collaborative Data Acquisition and Processing for Post Disaster Management and Surveillance Related Tasks Using UAV-Based IoT Cloud'. *International Journal of Ad Hoc and Ubiquitous Computing*, 34(4), 216-232.
 53. Semwal, S. K., & Saxena, R. S. (2019). 'CMOS Implementation of Time Delay Integration (TDI) for Imaging Applications: A Brief Review'. *IETE Technical Review (Institution of Electronics and Telecommunication Engineers, India)*.
 54. Sharma, S. K., Jain, K., & Suresh, M. (2019) Quantitative Evaluation of Panorama Softwares. In: *Vol. 500. Lecture Notes in Electrical Engineering* (pp. 543-561).
 55. Sholarin, E. A., & Awange, J. L. (2015) Photogrammetry. In. *Environmental Science and Engineering (Subseries: Environmental Science)* (pp. 213-230).
 56. Suh, J., & Choi, Y. (2017). 'Mapping Hazardous Mining-Induced Sinkhole Subsidence Using Unmanned Aerial Vehicle (Drone) Photogrammetry'. *Environmental Earth Sciences*, 76(4).
 57. Szeliski, R. (2007). 'Image Alignment and Stitching: A Tutorial'. *Foundations and Trends® in Computer Graphics and Vision*, 2(1), 1-104.
 58. Tanzi, T., Apvrille, L., Roudier, Y., & Dugelay, J.-L. (2014). 'UAVs for Humanitarian Missions: Autonomy and Reliability'.

59. Tareen, S. A. K., & Saleem, Z. (2018, 3-4 March 2018). 'A Comparative Analysis of SIFT, SURF, KAZE, AKAZE, ORB, and BRISK'. Paper presented at the *2018 International Conference on Computing, Mathematics and Engineering Technologies (iCoMET)*.
60. Tedim, F., Xanthopoulos, G., & Leone, V. (2015). 'Chapter 5 - Forest Fires in Europe: Facts and Challenges'. In J. F. Shroder & D. Paton (Eds.), *Wildfire Hazards, Risks and Disasters* (pp. 77-99). *Oxford: Elsevier*.
61. Tostevin, R. (2014). 'Hazards and the Himalaya'.
62. Vaidya, O. S., & Gandhe, S. T. (2018). 'The Study of Preprocessing and Postprocessing Techniques of Image Stitching'. Paper presented at the *2018 International Conference On Advances in Communication and Computing Technology, ICACCT 2018*.
63. Vautherin, J., Rutishauser, S., Schneider-Zapp, K., Choi, H. F., Chovancova, V., Glass, A., & Strecha, C. (2016). 'Photogrammetric Accuracy and Modeling of Rolling Shutter Cameras'. *ISPRS Annals of Photogrammetry, Remote Sensing and Spatial Information Sciences, III-3*, 139-146.
64. Wang, Z. B., & Yang, Z. K. (2020). 'Review on Image-Stitching Techniques'. *Multimedia Systems*, 26(4), 413-430.
65. Wierzbicki, D., Kedziński, M., & Fryskowska, A. (2015). 'Assesment of the Influence of UAV Image Quality on the Orthophoto Production'. Paper presented at the *International Archives of the Photogrammetry, Remote Sensing and Spatial Information Sciences - ISPRS Archives*.
66. Xu, Q., Chen, J., Luo, L., Gong, W., & Wang, Y. (2020). 'UAV Image Mosaicking Based on Multiregion Guided Local Projection Deformation'. *IEEE Journal of Selected Topics in Applied Earth Observations and Remote Sensing*, 13, 3844-3855.
67. Xu, S., Jiang, S., & Min, W. (2017). 'No-reference/Blind Image Quality Assessment: A Survey'. *IETE Technical Review (Institution of Electronics and Telecommunication Engineers, India)*, 34(3), 223-245.
68. Xu, Y., Ou, J., He, H., Zhang, X., & Mills, J. (2016). 'Mosaicking of Unmanned Aerial Vehicle Imagery in the Absence of Camera Poses'. *Remote Sensing*, 8, 204.

69. Yaacoub, J.-P., Noura, H., Salman, O., & Chehab, A. (2020). 'Security analysis of drones systems: Attacks, limitations, and recommendations'. *Internet of Things*, 11, 100218.
70. Yang, S., Shen, Z., Wang, X., Bai, T., Ji, Y., Jiang, Y., Liu, X., Dong, X., Li, C., Han, Q., Lu, J., & Xiong, G. (2018) UAV Assisted Bridge Defect Inspection System. In: *Vol. 539. IFIP Advances in Information and Communication Technology* (pp. 401-411).
71. Yu, M., Yang, C., & Li, Y. (2018). 'Big Data in Natural Disaster Management: A Review'. *Geosciences*, 8(5), 165.
72. Yu, R., Lyu, M., Lu, J., Yang, Y., Shen, G., & Li, F. (2020). 'Spatial Coordinates Correction Based on Multi-Sensor Low-Altitude Remote Sensing Image Registration for Monitoring Forest Dynamics'. *IEEE Access*, 8, 18483-18496.
73. Yue, G., Hou, C., Gu, K., Mao, S., & Zhang, W. (2018). 'Biologically Inspired Blind Quality Assessment of Tone-Mapped Images'. *IEEE Transactions on Industrial Electronics*, 65(3), 2525-2536.
74. Zhai, G., & Min, X. (2020). 'Perceptual image quality assessment: a survey'. *Science China Information Sciences*, 63(11).
75. Zhang, F., Yang, T., Liu, L., Liang, B., Bai, Y., & Li, J. (2021). 'Image-Only Real-Time Incremental UAV Image Mosaic for Multi-Strip Flight'. *IEEE Transactions on Multimedia*, 23, 1410-1425.
76. Zhang, Z. (2014). 'Camera Parameters (Intrinsic, Extrinsic)'. In K. Ikeuchi (Ed.), *Computer Vision: A Reference Guide* (pp. 81-85). Boston, MA: Springer US.
77. Zhao, G., Lin, L., & Tang, Y. (2013). 'A New Optimal Seam Finding Method Based on Tensor Analysis for Automatic Panorama Construction'. *Pattern Recognition Letters*, 34(3), 308-314.
78. Zhao, Y., Zhang, Y., Han, J., & Wang, Y. (2021) Analysis of Image Quality Assessment Methods for Aerial Images. In: *Vol. 1274 AISC. Advances in Intelligent Systems and Computing* (pp. 168-175).
79. Zhao, Y., Cheng, Y., Zhang, X., Xu, S., Bu, S., Jiang, H., Han, P., Li, K., & Wan, G. (2020). 'Real-Time Orthophoto Mosaicing on Mobile Devices for Sequential Aerial Images with Low Overlap'. *Remote Sensing*, 12(22), 3739.

80. Zhou, Y., Daakir, M., Rupnik, E., & Pierrot-Deseilligny, M. (2020). 'A Two-Step Approach for The Correction of Rolling Shutter Distortion in UAV Photogrammetry'. *ISPRS Journal of Photogrammetry and Remote Sensing*, 160, 51-66.
81. Zieliński, T. (2017). 'Unmanned Aircraft Systems In Support Of The Land Forces. Selected Issues'. *Journal of Science of the Gen. Tadeusz Kosciuszko Military Academy of Land Forces*, 184, 195-210.